European Cells and Materials Vol. 1. 2001 (pages 1-11) DOI: 10.22203/eCM.v001a01 ISSN 1473-2262

CHARACTERIZING FRETTING PARTICLES BY ANALYSIS OF SEM IMAGES

I. ap Gwynn* and C. Wilson
Institute of Biological Sciences, The University of Wales, Aberystwyth, Ceredigion, Wales, SY23 3DA

Abstract

Detailed surface characteristics of the particles produced during fretting may well be significant in determining their biological effects. Apart from a broad size determination very few attempts have been made at devising means of describing profile textures of particles. An approach is presented for describing the nature of particle shape and surface texture, as detected on the particle profile. Careful processing and analysis of the digitised image enabled both the sizes of micro-projections and their relative numbers to be determined. Such processing of images of a large number of particles generated a considerable amount of data. An artificial neural network was used to categorise the data and to compare the nature of fretting particles generated by titanium, titanium-molybdenum and stainless steel. Although showing a tendency towards a spherical form, all three metals produced different results, with titanium showing the greatest diversity of textures and sizes, steel the least.

Key Words: Fretting, particles, artificial neural networks, image analysis, fractal dimension, textural element, implants.

*Address for correspondence:
Iolo ap Gwynn
Institute of Biological Sciences
The University of Wales
Aberystwyth
Ceredigion
Wales SY23 3DA

E-mail: iag@aber.ac.uk
Telephone number: +44 1970 622324
FAX number: +44 1970 622350

Introduction

Cells respond to the physical presence of particles, in addition to any chemical products that arise from the particles' exposure to the physiological environment. As the physical features of particles, such as size, shape and surface texture can vary enormously, it is appropriate to ask the question; will such variations influence the response of the cell? Establishing effective protocols for quantifying the morphological features of particles is therefore a prerequisite to confronting this question

Particles initiate most biological responses as a consequence of their phagocytosis into immune system cells. The capacity to be phagocytosed imposes a size criterion on the particles that is likely to be a major determinant in biocompatibility. Shanbhag et al. (1994a) suggested a lower, as well as an upper size limit for phagocytosis to take place, and that the smaller diameter particles (<0.15μm) are less inflammatory than those which are >1.76 μm. They suggest that this difference reflects the two potential pathways of particle uptake: the smallest particles could be internalised by pinocytosis and the larger variety by phagocytosis. These two events have very different consequences on subsequent cell behaviour. As phagocytosis is the initial stage of an inflammatory response, it is accompanied by the release of various chemical mediators. Because pinocytosis is a routine cell activity, particles internalised in this way might not cause the secretion of such mediators. Oberdorster *et al.* (1994) describes an in *vivo* model in which particles are introduced into the pulmonary cavity of rats. The particles used in this case are composed of TiO_2 in two size groups, 250 nm and 20 nm. During the 1-year follow up period the smaller particles elicit a more persistent inflammation and impaired pulmonary macrophage function. Shanbhag *et al.* (1994b) noted that macrophage response, measured by mediator release, is dependent on the size of the dosed particulates *in vitro*. Also, hydroxyapatite particles only exhibit toxicity to cultured fibroblasts when dosed below the phagocytosable threshold (Evans, 1991). Gonzalez *et al.* (1996) noted a similar phagocytosability threshold, in an *in vitro* study estimating the mediator release from human macrophages exposed to Polymethylmethacrylate (PMMA).

It is also possible that more subtle shape and texture parameters may also influence either the tendency for a particle to be internalized, or the subsequent cell response. It is becoming increasingly apparent from a wide range of studies that cells are very responsive, in a tactile sense, to the environment in which they exist. Cell behaviour and phenotype may be influenced by the physical nature of the substrate upon which they are cultured or the extra-cellular

matrix in surrounding tissues (den Braber *et al.* 1995, 1996, Chesmel and Black 1995). In the orthopedic context, the textural nature of the biomaterial surface can dictate the nature of the implant/tissue interface. Some workers have investigated the effect of shape and texture on particle biocompatibility. Gelb *et al.* (1994) describes *in vivo* inflammatory response assays using PMMA particles of two kinds. Firstly, ground large fragments of PMMA with rough, irregular outlines and secondly, commercially obtained smooth PMMA spheres. Both particle groups have a similar population size profile. After preparation, the particles are tested in a subcutaneous rodent pouch model and the consequent inflammatory response estimated by assaying blood samples for various cytokines and white cell counts. Gelb *et al.* report that irregular shaped particles provoke a significantly greater inflammatory response as expressed by tumour necrosis factor-α, metalloprotease and prostaglandin E_2 levels as well as white cell counts. Although they demonstrate that shape and texture are possible determinants in particle biocompatibility, no attempt is made to quantify these features.

Particulate wear debris has been identified as a causal factor in a number of disease conditions associated with the use of orthopedic implants. Consequently, the nature of the wear debris is the subject of a number of studies: Shanbhag *et al.* (1994 b) examine particles of titanium alloy, steel and polyethylene retrieved from tissues during the revision of hip prosthesis. Size analysis of the scanning electron micrographs demonstrates a predominant (92%) sub micron distribution. Schmiedberg *et al.* (1994) use similar scanning electron microscopy techniques to examine particles produced in a vertebral disc prosthesis wear simulator. A similar, mainly submicron size distribution is noted and attempts at shape characterization of the particles are made. TiAlV fragments are described as "rough and irregular", CoCrMo, "irregular polyhedron" and forged CoCrMo as spherical. A comprehensive review of the existing literature describing the size and shape of wear debris is presented by Savio *et al.* (1994). Whereas many of the papers reviewed (over 200) provide precise size details, and some colloquial descriptions of morphology, none attempt quantifiable shape and texture estimates

A number of approaches to characterizing the shape or texture of objects have been published, in a variety of disciplines. Flook (1984) provides a useful comparison of the quantitative methods of shape characterization, namely form factors, Fourier analysis and fractal dimensions.

Form Factors

Form factors are dimensionless values generated by calculating a ratio of two simple geometric features. Fong (1978) uses the form factors "*chunkiness*" (width / length) and "*external compactness*" (diameter of embracing circle / diameter of circle of equivalent area) to describe shape changes in iron powder grains produced by various chemical reduction techniques. McKenzie *et al.* (1996) applies the "degree of roundness" ($[4\pi \times \text{area}] / \text{perimeter}^2$), to examine the shape of β-amyloid plaques in brain sections of Alzheimer's disease victims. A commonly applied image analysis routine, included in the proprietary image analysis software (PC_Image, *Foster Findlay*), used in the current study, applies the form factor "*circularity*" ($4 \times [\text{area} / \text{perimeter}^2]$) to estimate shape. In all cases actual size must also be considered, in addition to the form factor, for a meaningful description of an object.

Particle size analysis has been attempted in light (Case *et al.*,1994; Meachin *et al.,* 1973) and electron microscopical (Margevicius *et al.,* 1994; Maloney *et al.*, 1996) studies. Size is readily quantifiable in terms of area, radius or diameter. It is important to consider carefully the appropriate parameter with which to express size in light of the principal pathway by which particles normally exert any biological effects, namely phagocytosis. A number of workers, using particles of various sizes, have identified an increase in inflammatory potential for particles below the phagocytosable threshold (Evans, 1991; Gonzalez *et al.,* 1996; Shanbhag *et al.,* 1994a). It is generally accepted that phagocytotic cells can internalize spherical objects of up to 15-20μm in diameter. Irregularly shaped particles can also probably be internalized, as long as the longest axis (maximum feret diameter) does not exceed to same 15-20μm value. Expressing particles' sizes as area might lead to erroneous conclusions regarding potential biological effects as a rod shaped particle could have a similar diameter to a spherical one of a much smaller area. It is therefore more appropriate to present particle size as a longest diameter or length measurement. Literature describing orthopaedic wear debris does not provide any useful precedents for choosing a method for shape description (Savio *et al.*, 1994). However, Flook (1984) does suggest that form factors are an effective method for describing shape.

Textural analysis of particles

The term texture is taken to mean the two-dimensional outline of a particle profile. Texture has also been defined in terms of the one-dimensional surface characteristics of an image, by using grayscale, optical density values (McKenzie *et al.*, 1996). Several approaches are possible to provide this type of analysis.

Fourier or Harmonic Analysis

Fourier analysis describes the perimeter of the particle, using the centre of gravity as an origin, as a periodic function that is then expanded as a Fourier series. Flook (1984) notes that the Fourier method can describe particle shapes to a reasonable degree of accuracy but the number of harmonics required for the finest levels of detail would prove to be impractical to handle. One possible advantage to this approach is that a dimension related description is obtained. Investigators of fretting particles have not yet taken this approach. Recently however, the increased availability of powerful personal computers has made complex image processing and analysis procedures more accessible, and consequently worthy of consideration in this context.

Fractal Dimension

The Fractal Dimension (FD) is a value describing the shape filling capacity of a rough boundary. The concept of FD is based on the non-Euclidean system of geometry described by Mandelbrot (1982) and it has been used in a number of research applications. Whalley and Orford (1982) apply FD measurements to SEM images of sedimentary particles and Kaye (1986) employs similar

methods to the outline of fine powders. Keough *et al.* (1991), Smith *et al.* (1989), Landini and Rippin (1996) and Matsushita *et al.* (1991) study cell shapes. Calculating a FD for a given object is a complex procedure based upon measurement of perimeter in terms of decreasing units of measurement, and requires a significant amount of data processing. Although this is essentially a geometric measurement approach it is a method that can be modified for the processing of digitally stored images. Because this factor has been applied in a number of studies its application to fretting particle shape description was attempted in the present study.

Digital image analysis

It is a prerequisite of computer-based analysis that images are converted into a digital format. This has resulted in fundamental changes to image handling methodologies. Traditionally, microscopes (of light and electron designs) were fitted with conventional photographic devices for recording images of interest. Such images then needed to be scanned into a digital format for analysis. However, devices that collect digital images directly from cameras or microscopes are now in common use. Because they are stored in a numerical format, digital images can also be processed (contrast adjustment, sharpening, etc.) and analysed (quantification of areas, optical density, etc.). A digital image, or bitmap, represents an analogue image in a series of lines of pixels, which are stored as numbers. The quality of representation of the image is dependent on the number of pixels stored per line and number of lines in the digital image. The numerical value attributed to a pixel will vary. In a black and white (binary or 1-bit) image the pixel value can be only "1" or "0", representing white and black respectively, and the information is essentially two-dimensional. 8 bit grayscale images use 256 shades of gray including black (0) and white (255). 10, 12 or 16 bit images will store more levels of grayscale information for each pixel, respectively. There is considerably more information in the 256 gray levels of an 8 bit image than the 60, or so, that the human eye can separate. This information is however available for image analysis. For image analysis procedures the information in a grayscale image must normally be processed to define areas to be measured in the form of a binary image. This process is known as thresholding.

The main scientific advantage of computerized image analysis is the non-subjective manner in which information can be assessed. The computer can also detect contrast dependent information that is not always apparent to a human observer. The speed and repetitive potential of computers provide practical advantages that can facilitate the application of complex routines (such as fractal analysis), which would otherwise be impractical for collecting meaningful numbers of experimental replicates. Computer aided image analysis procedures can require image parameters that are different from those used in generating images for photographic reproduction. Images should emphasize the features of interest, on the basis of brightness contrast, in a way that makes them suitable for subsequent analysis procedures. This should be considered at the earliest stages of specimen preparation as well as in the choice of microscopy protocols to be applied.

Textural Elements (TE)

The collection of particle images in the digital format opens purely digital approaches to the description of image profile texture. This is the approach we have taken in developing a fundamentally new method to such texture description. We have called this the Textural Element (TE) method.

Although the Fractal Dimension provides an overall textural roughness factor, presenting the textural metric as a single value limits its descriptive potential and takes no account of variability in the surface components. It is also a scale independent descriptor. Scale independency is fundamental to fractal theory but in the case of fretting particles, knowing the specific size range of textural detail is important. The effect that particulates might exert on cells and tissues could well relate to the sizes of particle surface textural features. Cells normally lie in a size range of 5-30mm. Textural elements within this range, and smaller, are likely to influence cell behaviour. Therefore a textural description method that could analyse surface texture in terms of its size range was developed and its potential usefulness investigated.

In the TE method, surface projections (textural elements) of the particle profiles were identified. Successively larger textural elements were isolated in a sequence of "passes" until a complete profile of the particle surface features was built up. Three image-processing functions were used. These were, erosion, dilation and a logical XOR function. The method had two stages: Firstly, a particle outline was subjected to a sequence of erosions (passes), followed by a similar number of dilation passes, fine elements of surface detail were lost as a consequence of this process. Secondly, the resulting image was "subtracted" from the original image (a copy of which was retained in the computer memory for this purpose) using the logical XOR function. The result of this subtraction provided an image that contained only the TE, which had been removed during the original erosion/dilation sequence. Fine TE were detected at low numbers of erosion/dilation passes and larger TE isolated with more passes. By performing a sequence or passes of increasing magnitude it was possible to compile data describing the surface texture of the particle over a wide size range. For an accurate description it was necessary to filter out elements that were detected by more than one of the erosion/dilation sequences. In these cases only the record for the larger TE was retained, otherwise the number of finer TE were overestimated. Applying this method resulted in the acquisition of a substantial amount of multivariate data. Artificial neural network software was employed to examine the properties of that data, and relate it to the particle material of origin.

Generation of wear debris

Previous workers have obtained particles from two sources. Some have been isolated from tissues obtained during surgical replacement or revision of prosthesis (Campbell *et al.,* 1994, 1995; Lee *et al.,* 1992; Maloney *et al.,* 1995). Others have produced them by fretting wear simulators in the laboratory (Rogers *et al.,* 1993). In deciding which method of particle production would be appropriate for this study a number of criteria were

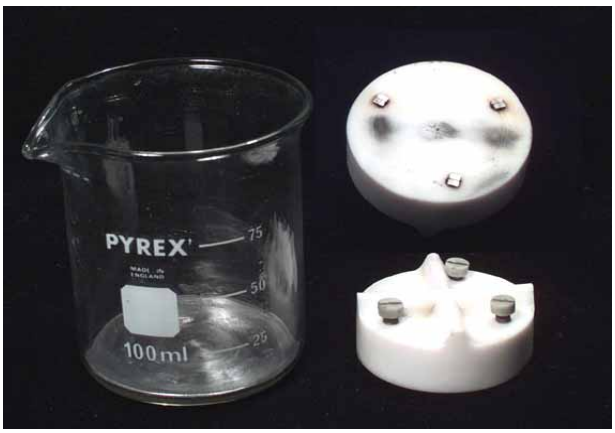

Figure1. Particle generating apparatus. A disc of the appropriate metal is attached to the base of the beaker, by means of adhesive. The Teflon magnetic stirrer follower was modified to hold three pins of the metal, whose height above the surface could be adjusted by turning the plastic screws.

considered. To perform a series of cell cultures with appropriate controls and replicates, in a related study, a large number of particles were required. For experimental integrity all particles used in comparable cell cultures should also be from the same batch of manufacture. A method that generated a large quantity of particles was therefore required. Particles would only be suitable for use in cell culture if they did not introduce any infectious agents. The method of particle production, therefore, had also to be sterile. Some experimental approaches required that the particles be produced under a variety of conditions. This feature was principally concerned with the suspending fluid into which the particles were produced. This could vary in terms of temperature, pH, protein and inorganic salt content. The most appropriate analogue of the *in vivo* situation was

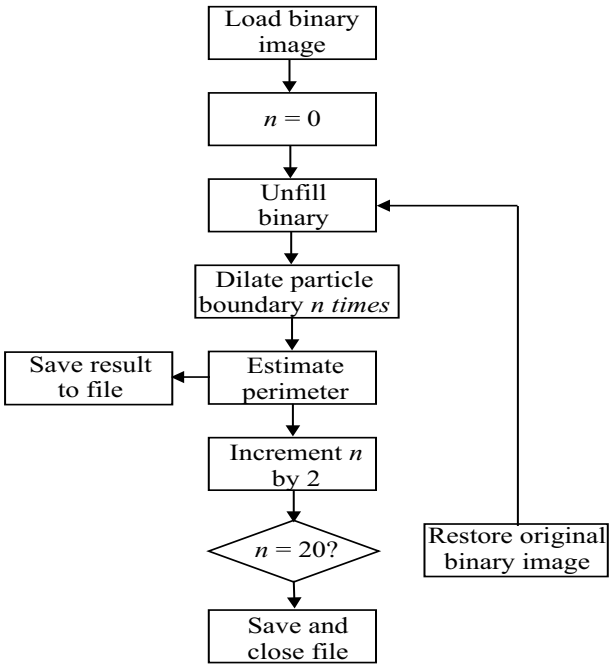

Figure 2. Flowchart describing the process by which the Flook (Boundary dilation) method is implemented in PC_Image.

to produce particles in a serum solution. Serum is a perishable substance, which will degrade after a few days in culture, the particle production method, therefore, had to be able to produce a sufficient volume of particulates within this time scale.

Particles were produced in a specially designed *in vitro* fretting simulator. Rogers *et al.* (1993) describes a laboratory fretting wear simulator for generating debris for experimental purposes. The system, using a rotating rod against a static disc, is based on the ASTM defined standard for wear simulators. Although, this method will produce large the amounts of debris, the incorporation of an electric motor into the system makes it difficult to sterilize. To facilitate the sterile production of particles a system was devised which used a laboratory magnetic stirrer and Teflon coated following head. The following head was studded on the underside with pins of the desired metal and then placed in a beaker, to the bottom of which a disc of the same type of metal was attached. The fluid to suspend the particles was placed in the beaker that could then be sealed and autoclaved as a closed unit. When placed on the magnetic stirring unit the metal pins rotated relative to the disc, causing liberation of wears debris into the suspending medium. After a sufficient number of particles had been produced, the beaker could then be unsealed under aseptic conditions and the particles removed.

Materials and Methods

Metals used

Three different types of implant quality metals were used in this investigation. Stainless steel was standard surgical implant specification for wrought 18 Chromium - 14 Nickel - 2.5 Molybdenum (ISO 5832/1). Standard implant-quality unalloyed titanium (CpTi - ISO 5832/2) was used. The titanium-molybdenum alloy had the formulation Ti-15Mo and was an experimental implant alloy.

Generation of particles

Particles were generated using a specially designed particle generator (Fig. 1). The generator was loaded with the Teflon follower and distilled water. The beaker, and its contents, was then placed on a conventional magnetic stirrer and the follower caused to rotate at a medium speed for periods of 24h or more, depending on the amount of particles required for an experiment. Particles for microscopic analysis were then removed and washed in distilled water. They were then stored in distilled water until required.

Microscopy

Standard SEM specimen mounting stubs were used to hold the samples. A smooth plastic Thermanox (polyethylene terephthalate) disc was attached to the upper surface of the stub. The surface of the disc was connected electrically to the aluminum stub by means of a drop of conductive silver paint. The particle suspensions were placed on the disc and the solvent was allowed to evaporate, so depositing the particles on the smooth surface. Apart from providing a smooth surface the plastic disc had the added advantage of improving imaging by providing the

metal wear debris with a smooth background against which they contrasted. The surface of the Thermanox was coated (after particles were dried on) with a thin film of evaporated carbon in a Polaron E3000 coating unit.

The optimal concentration of particles achieved a balance between having sufficient particles in each field of view so that one micrograph could provide a number of experimental replicates while avoiding clumping of the particles. The original particle suspension was centrifuged, in an ordinary bench centrifuge, and the supernatant water replaced with the same volume of absolute alcohol. As alcohol is more volatile than water the evaporation was faster, leaving less time for the aggregation of particles. In addition, as alcohol is a non-polar solvent it does not "bead" on the surface of the Thermanox disc. Applying ultrasound to the base of the SEM stub, and a flow of warm air over the surface, during the solvent evaporation also ensured effective dispersal of the particles.

The JEOL JSM840 SEM was used in secondary electron collection mode with standardized settings of 4kV accelerating voltage (to optimize edge resolution), 5mm working distance, to optimize resolution, and a magnification of 3,000. After setting brightness and contrast controls to provide the full contrast range the digital images were collected using a *KE Developments Printerface v. 2* frame grabbing software and board. Digital images of 650 x 764 pixels were stored of 50, randomly selected, fields of view. The images were archived to CD-ROM in the form of Windows bitmap image files.

Image Processing and Analysis

All image processing and analysis was carried out using PC_Image v2.2 (Foster Findlay) image analysis software, mounted on a personal computer. Applying Contrast stretching to all the images, before analysis, ensured that the full contrast range available in each grayscale image was made available for subsequent thresholding to binary. The grayscale level range to be selected for thresholding to form a representative binary image was set manually for each image to ensure selection of the complete outline of each particle. Some noise and artifactual components of the original grayscale image possessed the same gray values as the particles. Consequently these objects were included in the resulting binary as well as the desired particles. Binary image editing procedures were used to remove the unwanted components prior to measurements being taken of the detected objects. Objects below 30 pixels in size were filtered out of the data. Particles partially included at the edge of the image were eliminated. Large artifactual elements of the binary image that could not be distinguished automatically by size were eliminated manually.

Measurement and form factor

Calibration was performed in the PC_Image software on images of 1.1 μm diameter latex calibration spheres (Sigma), stored at exactly the same microscope settings as used for recording the particle images. The mean diameter of the latex spheres was found to be 42 pixels; therefore objects of 0.026μm were the smallest that could be

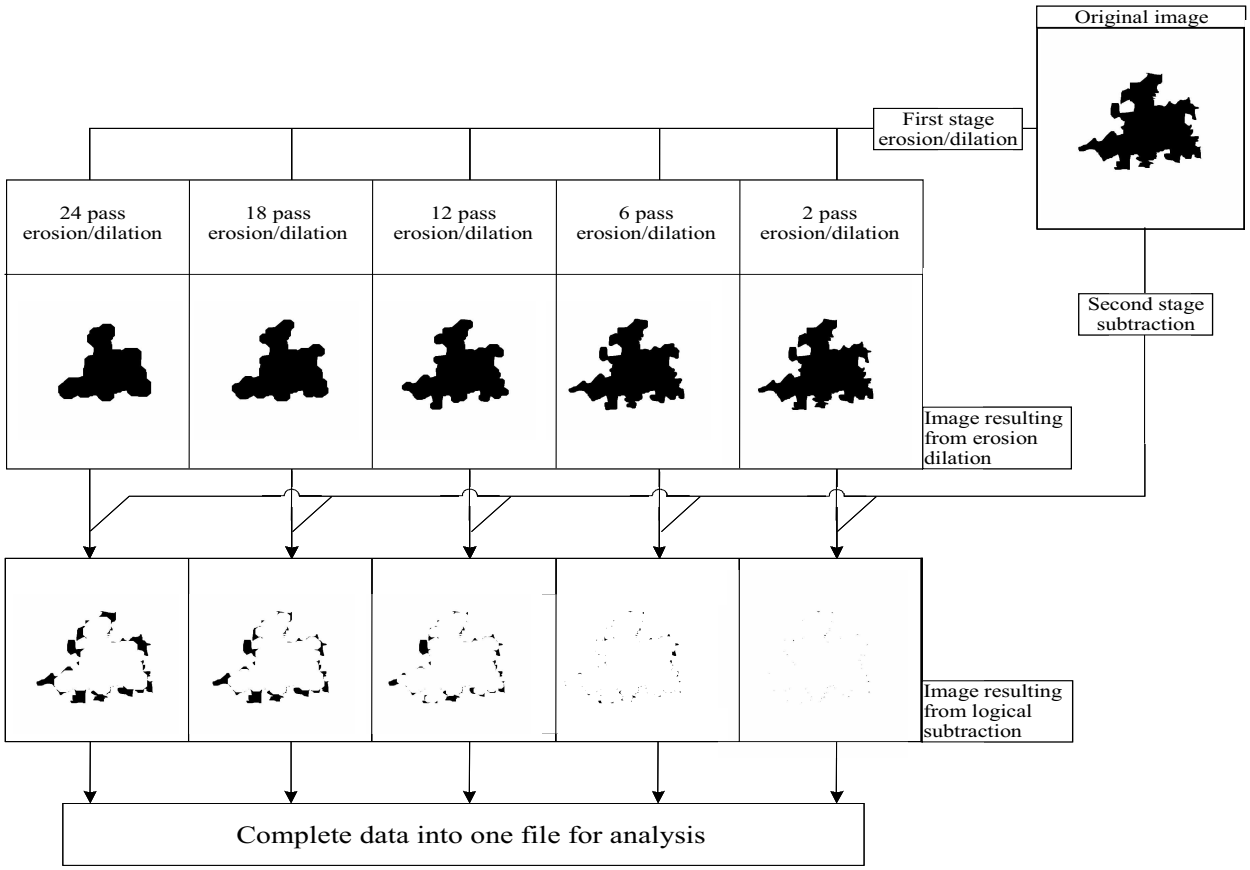

Figure 3. Demonstration of the use of erosion/dilation procedures and logical functions to isolate surface textural details of increasing size.

resolved, as single pixels, with this system.
The objects (particles) in the binary image were examined for size (diameter) and shape. The shape parameter chosen was circularity, defined as:

$$\text{Circularity} = 4 \times \frac{\text{area}}{\text{perimeter}}$$

The measured parameters for each particle were saved and finally transferred to Microsoft Excel 97 for further analysis.

Fractal Dimension

Fractal Dimension (FD) data was generated, using PC_Image, from digital images of wear particles by application of the Flook (1978) boundary dilation method to produce the data necessary for generating a Richardson plot. The process is illustrated in Fig.2. Consideration of possible curve break points and the calculation of final Fractal Dimension values was then carried out on the data, using Microsoft Excel. The process was automated within Excel by producing appropriate Visual Basic Macrocode. This provided an FD value for each particle.

Textural Elements (TE)

The procedure used to perform the complete analysis of a single particle profile, using PC_Image, is depicted in Fig.3. The data was then exported into a Microsoft Excel spreadsheet. Each particle's textural elements were classified, by percentage, into size categories. Checks for duplication of feature recognition were carried out, records for finer elements being eliminated from the data. Data for experimental groups and replicates within groups were compiled into a database. The database for particles from each metal type was then sorted by means of a Self Organizing Map (SOM) type of Kohonen type artificial neural network (ANN) (*Neuframe V3.0 - Neural Computer Sciences),* to determine if the differing patterns of surface texture were produced by particles of different types. The learning rate and neighbourhood parameters of 0.3 and 0.6 respectively were selected. A Visual Basic for Applications (VBA) macro, within Microsoft Excel, was composed to construct a visual representation of the grid from the *Neuframe* output file, the points that represented the data sets on the grid were reunited with their particle identities during this process. A logical depiction of the whole process to isolate TE is shown in Fig. 3.

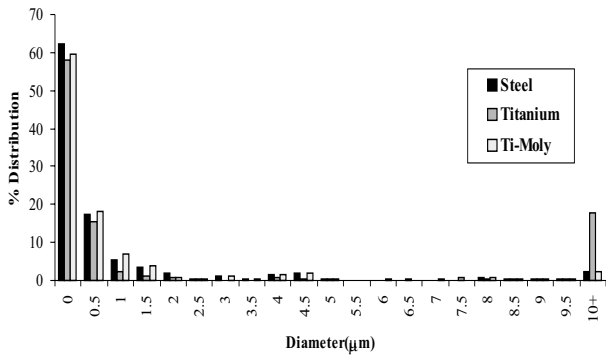

Figure 5. Size distribution of laboratory produced wear debris.

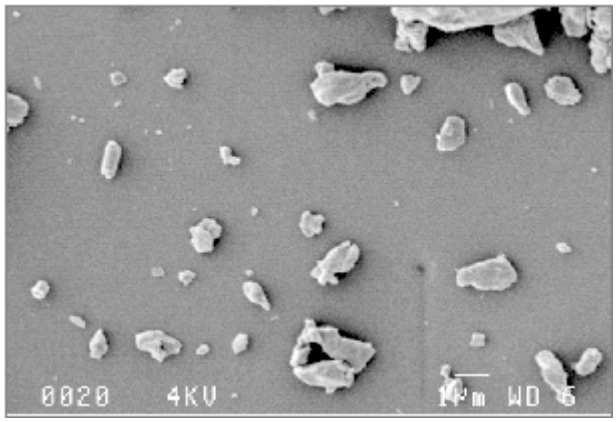

Figure 4. Scanning electron microscope image of Ti particle sample, as used for analysis procedures.

Results

SEM image (Fig. 4) shows the range of particle sizes that occured in the experimental samples. All of the measurements were made using images of this type. There was clearly an adequate difference in brightness between the specimen and the plastic Thermanox background for sufficient contrast to exist for effective image thresholding for image analysis.

Particle size classification

After compilation in a spreadsheet, the size data (maximum diameter) was categorized and expressed as percentage totals (Fig. 5). The greater proportion of all metal type particles were found to be in the sub 0.5 μm diameter category, with slightly more steel particles appearing to be in the smaller categories. A far greater proportion of titanium particles were in the greater than 10 μm diameter range.

Particle Shape Classification

The circularity measurement used by PC_Image was unstable when describing small objects. When applied to experimentally generated 'perfect' (within digital constraints) spheres, which should all have circularity value of 1, it was apparent that any object below 100 pixels in area was not suitable for shape evaluation by means of these protocols. Consequently, only those particles above the 100-pixel area threshold were evaluated. These were

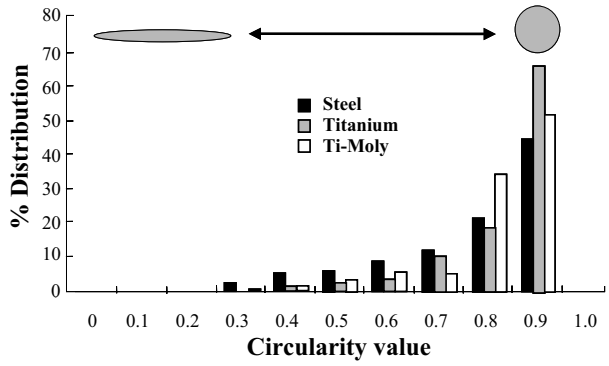

Figure 6. Classification data for the circularity values for particulate wear

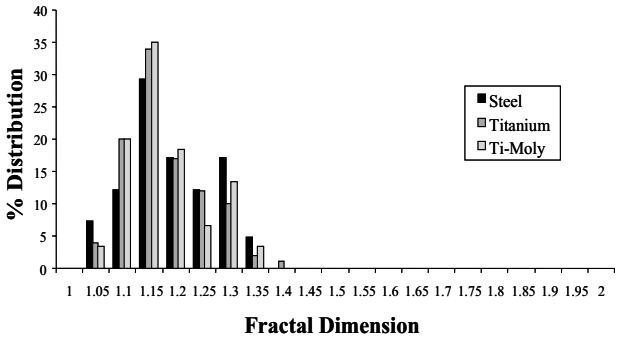

Figure 7. Classified Fractal Dimension Values for laboratory Produced Wear Debris

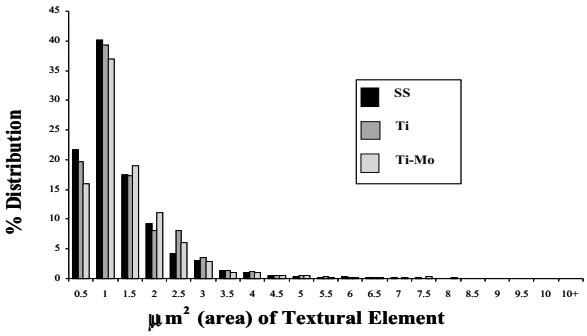

Figure 8. Distribution of Textural Elements Classified into μm^2 size categories

equivalent to 0.068μm^2 (equivalent circle diameter of 0.29μm) particles. Therefore only the largest particles were considered, but as the form factor was more likely to be significant in determining the response of cells this was considered to be acceptable. In order to analyse the smaller particle range reliably a microscope with a higher resolving power would have to be used. The results are presented in Fig. 6. For all metal types, the more rounded profile predominated, with titanium appearing to produce a more spherical profile than the other metals.

Fractal Dimension determination

Different patterns of distribution could be seen between the metal particles in the different fractal dimension categories (Fig. 7). Whereas stainless steel predominated in the FD1.05 and 1.3 categories, the titanium and titanium / molybdenum were more prevalent in the FD1.1 and 1.15 types. Only titanium particles appeared to generate values of FD1.4. The greater proportion of the particles, of all three metal types, fell into the FD1.15 category. The relative closeness of the variations suggested that the differences between the metals were subtle rather than dramatic.

Textural Element deduction

Graphical representation of the distribution of the pooled textural element description of the different metal particles is presented in Fig.8. The total numbers of, randomly selected, particles analyzed were 46, 119 and 64 for steel, titanium and Ti-Mo, respectively. A small tendency for larger textural elements to predominate was deduced subjectively from the data. This would suggest that the titanium and titanium / molybdenum particles were slightly 'rougher' than the steel ones. However, interpretation of such raw multivariate data is difficult.

To address the question of whether different metals produced particles of distinctly different textural profiles, the data was examined by the SOM ANN to attempt to identify inherent patterns. To test this approach control shapes of known defined textures were processed using the same method. Should the system have been unable to distinguish between such control-textures it was unlikely that classification of naturally occurring textures would be successful. 5 control textures were used and applied to objects of the same shape. 36 objects of each texture were replicated with slight variation in perspective and orientation, resulting in a database of 5×36=180 shapes. The database resulting from TE analysis of these objects was presented to the SOM ANN. Clear classification was achieved on a 10×10 grid with algorithm settings of *Learning Rate* and *Neighborhood* parameters of 0.3 and 0.6, respectively. The map presented in Fig 9 shows the patterns reported by the ANN. Clear distribution based on texture differences was achieved. Groups are encircled to illustrate that categorization. The metal particle shape database consisting of the particle textures was then subjected to the same procedure (Fig.10). The resultant pattern was, not surprisingly, more complex than that obtained with the regularly defined control objects. Titanium particles were distributed into 67 different categories, 28 of them exclusive. Only 4 stainless steel particles, and 8 titanium / molybdenum, were placed in exclusive categories. There was a clear indication that Ti produced a far greater range of surface textures than Ti-Mo and steel, respectively. By selecting the categories where metal particles were placed more than once, and eliminating single occurrences, there was, once more, a strong suggestion that each metal produced a distinctly different pattern. Titanium was distributed over a broad range of categories Titanium / molybdenum showed a distinct grouping and stainless steel was restricted in its distribution (Fig.11).

Discussion

The digital approach to the analysis of micrographs, of artificially produced fretting particles, proved effective for analyzing the large numbers of replicate data produced. Analogous studies (reviewed by Savio *et al.* 1994) that examined micrographs manually do not include as much data as the present study. As wear debris *in vivo* is likely to produce particles in huge numbers, obtaining a respectable population sample is important to produce dependable results. However, once established, the techniques described here could be carried out on relatively small numbers of particles to provide useful indicators of potential biocompatibility problems.

A number of workers have attempted size classification of wear debris obtained both *in vitro* and *in vivo*. The evidence that wear debris produced by fretting processes exists in the sub micron size range (Case *et al.*, 1994; Meachin *et al.,* 1973; Margevicius *et al.,* 1994; Maloney *et al.,* 1995,1996) was confirmed for each of the metals investigated (Steel – 79.7%, Ti – 63.8%, Ti-Mo – 77.9%). Previous studies suggest that submicron particles

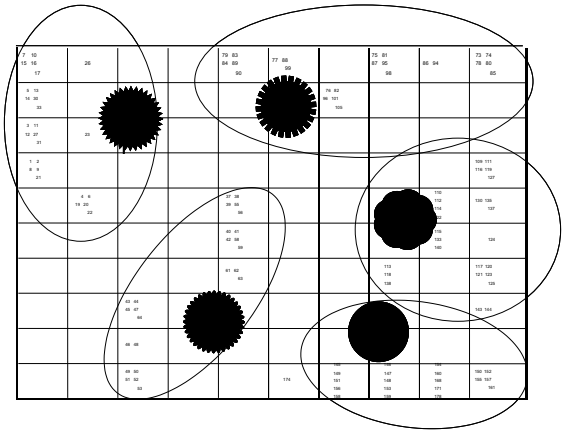

Figure 9. Test of the distribution of data generated by the TE analysis of five artificially created textures to objects, as categorized by the SOM ANN. Five distinct distribution groups have been detected.

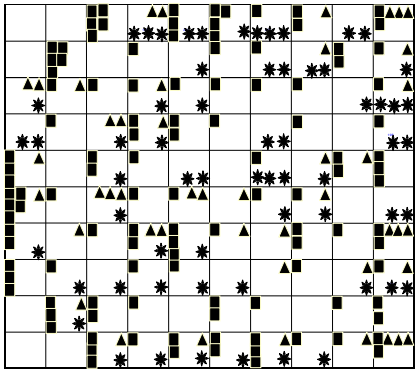

Figure 10. TE data grid, as distributed by a Kohonen SOM ANN, for stainless steel (triangles), titanium (squares) and titanium molybdenum (stars) particles. Stainless steel (n46) in 33 categories (4 exclusive), titanium (n119) in 67 categories (28 exclusive), titanium / molybdenum (n64) in 44 categories (8 exclusive).

show an inflammatory potential (DiCarlo and Bullough, 1992; Gelb *et al.,* 1994). However, this does not always seem to be the case and larger particles may also be implicated. A thorough analysis of particle shape and texture is therefore necessary.

Meaningful correlation of the results presented here with previously observed shape data is more difficult due to the subjective way in which most previous studies have described shape. Our results, indicating a broadly spherical outline to the metallic particles generated, confirmed the qualitative description given elsewhere to metallic debris as having a greater tendency to form more 'globular' structures than do polymeric or ceramic particles (Savio *et al.,* 1994). Despite its limitations at the lower size range the circularity measurement showed that the metals studied did show circularity values close to 1 – that expected of the outline profile of a perfect sphere. Many of the studies which Savio *et al.* reviews, which suggested that metallic particles had a 'globular' profile, had been performed on wear debris retrieved from *in vivo*. This, as well as the correlation with the size data, suggests that the wear debris generator developed for this study, produced particles that resembled closely those obtained from fretting biomaterials *in vivo*. It also suggests that experiments where such particles might be administered either to cells *in vitro* or to tissues *in vivo,* for experimental purposes, the results should follow those to be expected in implant fretting situations. It also has the advantage of being easily duplicated, as well as enabling the production of sterile particles.

Analysis of digital images needs to be carried out with some caution, as the pixilated nature of the image can lead to erroneous conclusion in certain circumstances. Examination of the size data showed that the distribution did not return to zero for the smallest particles. Calibration of the system with latex spheres suggested that the effective resolution limit was about 0.026µm. However at this level of a single pixel particles were indistinguishable from noise. Consequently, it was found to be appropriate to eliminate objects with an area below 30 pixels (assuming spherical morphology, diameter = 0.1 µm). The circularity factor calculation also became unstable when considering objects that are smaller than this. A complete description of the population size profile would require working with higher resolution images. However, the biological effects of particle surface textural variation were more likely to be important in particles within the size range studied. Some caution may be required in the interpretation of the results in terms of their actual significance, because the method of deposition of the particles onto a flat surface may result in asymmetric particles being oriented in a preferred way during the deposition procedure. Alternative approaches to imaging the particles to ensure completely random orientation may be required to obtain accurate results. On the other hand this aspect of particle behaviour may have no significance whatsoever.

The observation that titanium produced significant numbers of particles above 10 µm diameter provides grounds for some speculation regarding clinical observations associated with the use of pure titanium devices. Dark pigmentation of tissue surrounding titanium devices is well known. Particles in the phagocytosable size range can be disseminated from the implant site within phagocytes (Case *et al.,* 1994). It is probable that particles above this size range accumulate at the site of the implant, resulting in the observed pigmentation. However, as titanium has inferior erosion resistance to the other metals, the observed tissue loading with this metal could just as easily be a quantitative effect.

Higher resolution images could be analyzed to describe the size profile of the entire population and also permit accurate shape quantification of the smallest particles. Such images would need to be obtained on a microscope with a higher resolving power than was available for the current work, such as a Field Emission SEM. However, as the range of particle sizes found in the population of fretting debris spanned a number of orders of magnitude, it might be appropriate to use a number of different magnifications when preparing micrographs of such populations. Accurate calibration of each magnification used would be required to ensure accurate integration of the results into the

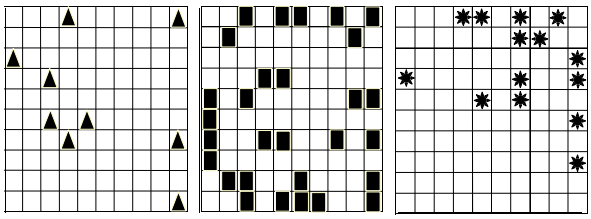

Figure 11. TE data grids of stainless steel, titanium and titanium / molybdenum showing only those categories where metal particles were placed by the SOM ANN in more than a single case.

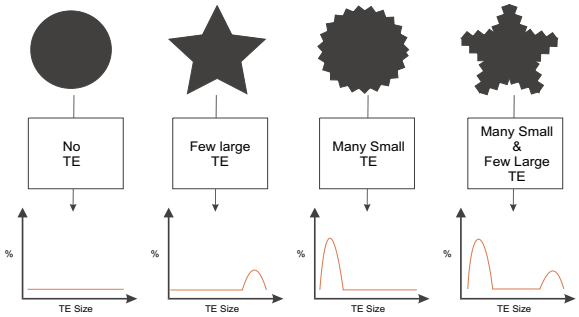

Figure 12. Classification of artificially created objects, showing expected distribution of textural elements

complete experiment database. Also, when using images of different magnifications care would be needed, when selecting areas to be imaged, to ensure that a representative sample of the heterogeneous population was being examined. However, the basic approach described here would be applicable at all magnifications.

In order to investigate the possible role of large titanium particles in tissue pigmentation, tissue samples could be retrieved, the metal content extracted and prepared for microscopy. The image analysis procedure described could then be applied to determine the size and texture profile of the particles. If large particles were being retained at the site of the pigmentation then the population size profile would be different from the heterogeneous population observed in this study, and a possible size-based discriminatory behaviour of the tissue phagocytes assessed. The effect of particle surface texture could also be studied in this way.

Both the established Fractal Dimension (FD) and the novel Textural Element (TE) technique, for describing outline texture, provided some useful information for comparisons to be made between the different metal types. Small proportions of the particle population, especially in the case of titanium, appear to show significantly different FD values. It is not possible, at the present moment, to identify the significance, if any, of such results. However, we have demonstrated a useful new method for characterizing surface textures of particles, which would be useful to apply to particles retained during tissue discoloration or from the lungs. Any possible discriminatory behaviour of tissue phagocytes on the basis of surface texture could then be tested.

The basis of TE analysis is most easily explained by reference to Fig.12. Clearly, large projections from the surface of the particle will record as large elements. Small projections will be listed as small elements. Also smaller projections on the surface of larger ones should also be recorded. A complete profile of all the surface projections is generated. Some care is required when analyzing the data generated by the image analysis software. The co-ordinates recording the position of each particle must be retained, and used to check for duplication of records, in the results of different erosion/dilation passes. This check must be carried out otherwise an over-estimate of the number of small elements may be obtained. A very large number of data point are accumulated to describe each particle, which was difficult to analyse in its raw form. Some indication is given of differences between the metals by a crude compilation of the data into a chart (Fig.8). Artificial neural networks are now well established as a means of identifying patterns in and comparing such large multivariate data sets (Hurst *et al.,* 1997; Fukushima, *et al.* 1997; Marabini and Carazo, 1994, Eastham and ap Gwynn, 1997). A Kohonen type of Self Organizing Map (SOM) was used in this study.

Several stages of data processing were necessary to transfer the image analysis data of the TE, first of all into a spreadsheet, for rearrangement into a suitable form for input into the neural network software. The SOM has no prior 'knowledge' of the identity of the type of particle represented by a particular set of data. Output from the ANN was in the form of a 2 dimensional grid onto which points representing the textural data sets were placed. The proximity of each point relative to the others is dependent on similarities (or dissimilarities) in the underlying data. The ANN program, Neuframe, accepts and produces data output compatible with a Microsoft Excel™ spreadsheet. Following a training session, using Neuframe, the resulting attempt at distribution of the data could be exported as a text file, which could be processed using Excel. A Visual Basic for Applications (VBA) macro, within Excel, was written to automate the arrangement of the data into a distribution map. Such a process can be time consuming, but does provide data that would not otherwise be available. One of the major difficulties with the application of artificial neural networks to data processing is that there is no direct check on the accuracy, or otherwise of the results. Only by testing known data against the system can confidence in the system be gained. For this reason the series of artificially produced test images that were analyzed in exactly the same way as the experimental particles provided useful evidence of the effectiveness of SOM for sorting similar data (Fig.9). The result is not always immediately obvious, as a cursory examination of Fig 10 would suggest. However, by carefully filtering the data to accept only recurring patterns (Fig 11) a clear difference between the metal particle types emerges. Whether these differences were significant in terms of the biological response to such particles was outside the scope of the current study. Although elaborate to set up initially, once the computing stages are automated then reasonably rapid analysis of microscopic images is possible in this way. This provides some interesting new

avenues for future research into the relationship between particle surface textures and cellular responses to it, both *in vitro* and *in vivo*.

Acknowledgements

Titanium and Steel samples were obtained from the AO Research Institute, Davos. These metals were as used for orthopaedic implants in currently clinical use. The Titanium Molybdenum alloy, which is currently being evaluated as a potential implant material, was supplied by J Disegi of *Synthes*, Paoli, PA, USA. This work was supported by the AO/ASIF Research Commission, Bern (project No. 96-G7).

References

Campbell P, Ma S, Schmalzried T, Amstutz HC. (1994) Tissue digestion for wear debris particle isolation. J Biomed Mat Res **28**: 523–526.

Campbell P, Ma S, Yeom B, McKellop H, Schmalzried TP, Amstutz HC (1995) Isolation of predominantly submicron-sized UHMWPE wear particles from periprosthetic tissues. J Biomed Mat Res **29**: 127–131.

Case CP, Langkamer VG, James C, Palmer MR, Kemp AJ, Heap PF, Solomon L. (1994) Widespread dissemination of metal debris from implants. J Bone and Joint Surg Brit **76b**: 701–712.

Chesmel KD, Black J. (1995) Cellular-responses to chemical and morphologic aspects of biomaterial surfaces . 1. A novel *in-vitro* model system. J Biomed Mat Res **29**: 1089–1099.

denBraber ET, deRuijter JE, Smits HTJ, Ginsel LA, von Recum AF, Jansen JA. (1995) Effect of parallel surface microgrooves and surface energy on cell growth. J Biomed Mat Res **29**: 511–518.

denBraber ET, deRuijter JE, Smits HTJ, Ginsel LA, vonRecum AF, Jansen JA. (1996) Quantitative-analysis of cell-proliferation and orientation on substrata with uniform parallel surface micro-grooves. Biomaterials **17**: 1093–1099.

DiCarlo EF, Bullough PG. (1992) The biological responses to orthopaedic implants and their wear Debris. Clin Mat **9**: 235–260.

Eastham A, ap Gwynn I (1997) Archaeology and the electron microscope. Eggshell and neural network analysis of images in the Neolithic. Anthropozool **25-26**: 85–93.

Evans EJ (1991) Toxicity of hydroxyapatite *in vitro* – The effect of particle-size. Biomaterials **12**: 574–576.

Flook AG. (1984) A comparison of quantitative methods of shape characterisation. Acta Sterol **3/2**: 159–164.

Flook AG. The use of dilation logic on the Quantimet to achiebve fractal dimension characterisation of textured and structured profiles. Powder Technol **21**: 295–298.

Fong FT, Beddow JK, Vetter AF. (1978) A technique to show effects of a chemical reaction upon particle morphology. *in* Proceedings of the Powder and Bulk Solids Conference, Rosemont, Illinios, Cahners Explosion Group.

Fukushima N, Shinbata H, Hasebe T, Yokose T, Sato A , Mukai K. (1997) Application of image analysis and neural networks to the pathology diagnosis of intraductal proliferative lesions of the breast. Jap J Canc Res **88**: 328–333.

Gelb H, Schumacher HR, Cuckler J, Baker DG. (1994) *In-vivo* inflammatory response to polymethylmethacrylate particulate debris - effect of size, morphology, and surface-area. J Orthop Res **12**: 598.

Gonzalez O, Smith RL, Goodman SB. (1996) Effect of size, concentration, surface-area, and volume of polymethylmethacrylate particles on human macrophages *in-vitro*. J Biomed Mat Res **30**: 463–473.

Hurst RE, Bonner RB, Ashenayi K, Veltri RW, Hemstreet GP (1997) Neural net-based identification of cells expressing the P300 tumor-related antigen using fluorescence image analysis. Cytometry **27**: 36–42.

Kaye BH. (1986) The description of two-dimensional rugged boundaries in fine particle science by means of fractal dimensions. Powder Technol **46**: 245–254.

Keough KMW, Hyam P, Pink DA, Quinn B. (1991) Cell-surfaces and fractal dimensions. J Microsc **163**: 95–99.

Landini G, Rippin JW (1996) How important is tumour shape? Quantification of the epithelial connective tissue interface in oral lesions using local connected fractal dimension analysis. J Pathol **179**: 210–217.

Lee JM, Salvati EA, Betts F, Dicarlo EF, Doty SB, Bullough PG. (1992) Size of metallic and polyethylene debris particles in failed cemented total hip replacements. J Bone Joint Surg Brit **74**: 380–384.

Maloney WJ, Smith RL, Schmalzried TP, Chiba J, Huene D, Rubash H. (1995) Isolation and characterization of wear particles generated in patients who have had failure of a hip-arthroplasty without cement. J Bone and Joint Surg Amer **77**: 1301–1310.

Maloney WJ, James RE, Lanesmith P. (1996) Human macrophage response to retrieved titanium alloy particles *in vitro*. Clin Orthop and Relat Res **332**: 268–278.

Mandelbrot BP (1992) *in* The Fractal Geometry Of Nature. WH Freeman, San Francisco.

Margevicius KJ, Bauer TW, Mcmahon JT, Brown SA , Merritt K. (1994) Isolation and characterization of debris in membranes around total joint prostheses. J Bone and Joint Surg Amer **76a**: 1664–1675.

Matsushita M, Ragnarson B, Grant G (1991) Topographic relationship between sagittal purkinje-cell bands revealed by a monoclonal-antibody to zebrin-I and spinocerebellar projections arising from the central cervical nucleus in the rat. Exp Brain Res **84**: 133–141.

McKenzie JE, Roberts GW, Royston MC (1996) Quantification of Alzheimer-type neurofibrillary lesions by automated image analysis. Neurodegeneration **5**: 251–258.

Meachin G, Williams DF (1973) Changes in nonosseous tissue adjacent to titanium implants. J Biomed Biomat Res **7**: 555–572.

Oberdorster G, Ferin J, Lehnert BE. (1994) Correlation between particle size, *in vivo* particles persistence and lung injury. Environ Health Perspect **102**: 173–179.

Rogers SD, Pearcy MJ, Hay SJ, Haynes DR, Bramley

A , Howie DW. (1993) A method for production and characterization of metal prosthesis wear particles. J Orthop Res **11**: 856–864.

Savio JA, Overcamp LM, Black J. (1994) Size and shape of biomaterial wear debris. Clinical Materials **15**: 101–147.

Schmiedberg SK, Chang DH, Frondoza CG, Valdevit ADC , Kostuik JJ (1994) Isolation and characterization of metallic wear debris from a dynamic intervertebral disc prosthesis. J Biomed Mat Res **28**: 1277–1288.

Shanbhag AS, Jacobs JJ, Black J, Galante JO, Glant TT (1994a) Macrophage/particle interactions – effect of size, composition and surface-area. J Biomed Mat Res **28**: 81–90.

Shanbhag AS, Jacobs JJ, Glant TT, Gilbert JL, Black J, Galante JO. (1994b) Composition and morphology of wear debris in failed uncemented total hip-replacement. J Bone and Joint Surg Brit **76B**: 60–67.

Smith TG, Marks WB, Lange GD, Sheriff WH, Neale EA (1989) A fractal analysis of cell images. *J. Neurosci. Meth.* **27** 173–180.

Whalley WB, Orford JD (1982) Analysis of scanning electron-microscopy images of sedimentary particle form by fractal dimension and Fourier-analysis methods. Scanning Electr Microsc **1982(P2)** 639–647.

Discussion with Reviewers

A. Wennerberg: The usage of Richardson plots for the determination of FD is a bit unclear.
Authors: As we are simply applying a well-established technique, with the full details already published by the original authors we feel it is not necessary to include all the details in the text of this paper. Interested readers are referred to the original papers.

A. Wennerberg: Fractal Dimension: How significant are the found differences in fractal dimensions compared with the uncertainty in the calculation of FD?
Authors: This is precisely the type of problem involved with the use of FD, as is the non-dimensional nature of the factor. Our inclusion of the data is intended to raise questions as to the validity of its use in this context, without an allowance being made for the scale of measurements made. Although it might be convenient to reduce the perimeter profile of a particle to a single number, we feel it is an over simplified descriptor and therefore not possessing sufficient resolution to enable a useful definition of particle profile texture to be made. It was for this reason that we resorted to developing the alternative, but much more complex approach of the Textural Element analysis. This we feel, with the added facility of artificial neural network processing of the data has the potential to discriminate between different profile textures at a very high resolution.

A. Wennerberg: How significant is the difference in just taking into account the categories with more than two occurrences of the different materials in the individual boxes compared to adding boxes with the single occurrence? The picture changes considerably and the conclusions may be a bit less obvious.
Authors: The main purpose of this illustration was to demonstrate that there were differences between the metal types in terms of the range of particle shapes they produced. Clearly, these categories with more than occurrence indicate a greater tendency to produce particles of such types. The different metals do seem to exhibit different patterns. The wider range of shapes that seem to be produced by the titanium could well be significant. Only future testing can confirm that.

M. Textor: The particle distribution may be linked to the metallurgical state, not just the type of metal. In particular it may be interesting for the future to look once into the composition of the particles (e.g. by SEM/EDS) in the different size ranges. For alloys such as α-β alloys TIAlV or TiAlNb, it could well be that the particle size and/or form are also linked to the size and properties of the two phases in the system.
Authors: We agree. This is an aspect that warrants being tested. This emphasises the potential power of the Textural Element analysis to distinguish between the types of particles that are produced by different metals in different metallurgical states. The biological significance of any such differences have yet to be established. However, by using this tool it should be possible to test such an hypothesis.